molbank

MDPI

Short Note

Dichloro[2,5-bis(diisopropylphosphorimidoyl-κ*N*-(4,6-dimethylpyrimidine-κ*N*))pyrrole-κ*N*]yttrium(III)·toluene

Emily L. Trew, David Szucs and Paul G. Hayes *

Canadian Centre for Research in Advanced Fluorine Technologies (C-CRAFT) and Department of Chemistry and Biochemistry, University of Lethbridge, 4401, University Drive West, Lethbridge, AB T1K 3M4, Canada; e.trew@uleth.ca (E.L.T.)

* Correspondence: p.hayes@uleth.ca

Abstract

The compound dichloro[bis(diisopropylphosphorimidoyl-κ*N*-(4,6-dimethylpyrimidine-κ*N*))pyrrole-κ*N*]yttrium(III) was synthesized from one equivalent of NaL [L = 2,5-[^{i}Pr$_2$P=N(Pym^{Me})]$_2$NH(C$_4$H$_2$); Pym^{Me} = 4,6-dimethylpyrimidine] and YCl$_3$(THF)$_{3.5}$ and crystallized from toluene. X-ray quality crystals of LYCl$_2$ were obtained with one toluene solvent molecule in the asymmetric unit. The geometry, bond lengths and angles were analyzed and found to contain similar parameters to comparable structures in the literature, and the product was further characterized by NMR spectroscopy. To the best of our knowledge, this is the first reported seven-coordinate Y(III) complex supported by a pentadentate ligand wherein all five donor atoms are nitrogen.

Keywords: rare earth metal; yttrium; X-ray crystal structure; pentadentate ligand; iminophosphorane; bisphosphinimine; pyrrole; pyrimidine

1. Introduction

Rare earth (RE) metal complexes, including those of yttrium, can be highly reactive due to their substantial Lewis acidity compared to their transition metal counterparts [1]. Previously, the Hayes group reported thermally unstable bisphosphinimine carbazole-based pincer-supported lutetium complexes that underwent undesired cyclometallation reactions, resulting in complexes that exhibited reduced small molecule reactivity [2,3]. Following that work, the thermally robust bisphosphinimine pyrrole-based lutetium complex (2,5-[Ph$_2$P=N(4-^{i}PrC$_6$H$_4$)]$_2$N(C$_4$H$_2$))Lu(CH$_2$SiMe$_3$)$_2$, was isolated [4] and utilized to synthesize (2,5-[Ph$_2$P=N(4-^{i}PrC$_6$H$_4$)]$_2$N(C$_4$H$_2$))Lu(CH$_2$SiMe$_3$)(NHCPh$_3$), which was further studied for its reaction chemistry [5]. Although stabilizing well-behaved RE complexes can be challenging, fine-tuning the ancillary ligand architecture can inhibit cyclometallation reactions, providing species that mediate remarkable chemical transformations. For example, complexes that contain multiple bonds between the central rare earth metal and a main group element (i.e., C, N, Si, P, etc.) are often sought for potential use in novel catalytic and stoichiometric reactions [6–11]. Recently, the Hayes group reported a monoanionic pentadentate ligand, L$^-$ [L = 2,5-[^{i}Pr$_2$P=N(Pym^{Me})]$_2$NH(C$_4$H$_2$); Pym^{Me} = 4,6-dimethylpyrimidine], which was able to support RE (i.e., Lu) chlorides [12]. They were targeted as possible precursors to unusual RE-imido complexes [8,9].

In this work, the molecular and crystal structure of dichloro[bis(diipropylphosphorimidoyl-κ*N*-(4,6-dimethylpyrimidine-κ*N*))pyrrole-κ*N*]yttrium(III)·toluene (LYCl$_2$·toluene) is examined (Scheme 1). This structure has been established using X-ray crystallography and

check for updates

Academic Editor: Kristof Van Hecke

Received: 12 September 2025
Revised: 25 September 2025
Accepted: 29 September 2025
Published: 30 September 2025

Citation: Trew, E.L.; Szucs, D.; Hayes, P.G. Dichloro[2,5-bis(diisopropylphosphorimidoyl-κ*N*-(4,6-dimethylpyrimidine-κ*N*))pyrrole-κ*N*]yttrium(III)·toluene. *Molbank* **2025**, *2025*, M2066. https://doi.org/10.3390/M2066

multinuclear NMR spectroscopy. Studying the geometry and bonding within rare earth complexes, such as $LYCl_2$, is important because that information can provide key insights with respect to potential reactivity, and thereby, applications.

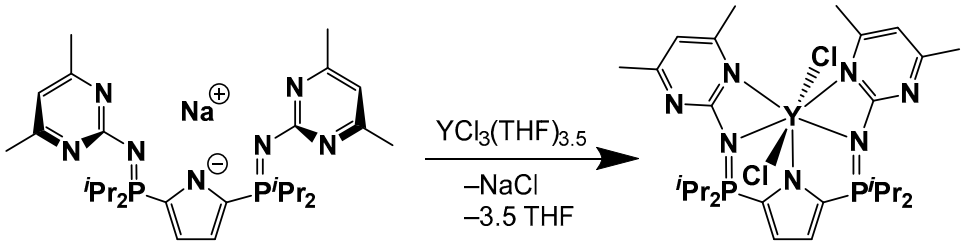

Scheme 1. Synthesis of $LYCl_2$.

2. Results

2.1. Structural Commentary

The title compound, $LYCl_2$·toluene, contains one yttrium (III) ion supported by a monoanionic pentadentate ligand, L, along with two chlorides (Figure 1). The complex has 2-fold molecular rotation symmetry with the 2-fold axis containing the Y1–N4 bond, but crystallizes at a general position. The geometry at yttrium is distorted pentagonal bipyramidal, highlighted by the five nitrogen donors being in the same plane (P1–N3–C6–N1 torsion angle = 173.5(2)°, P2–N5–C23–N7 torsion angle = 174.3(2)°, N3–P1–C13–N4 torsion angle = −5.1(2)°, N5–P2–C16–N4 torsion angle = 3.9(2)°) and the Cl1–Y–Cl2 angle (161.81°) approaching the ideal value of 180°. Other selected bond lengths and angles are included in Table 1 (please refer to Supplementary Materials for additional information). The geometry, bond distances, and angles are similar to those within the related lutetium complex, $LLuCl_2$ [12], reinforcing the similarities in L-supported RE metal complexes.

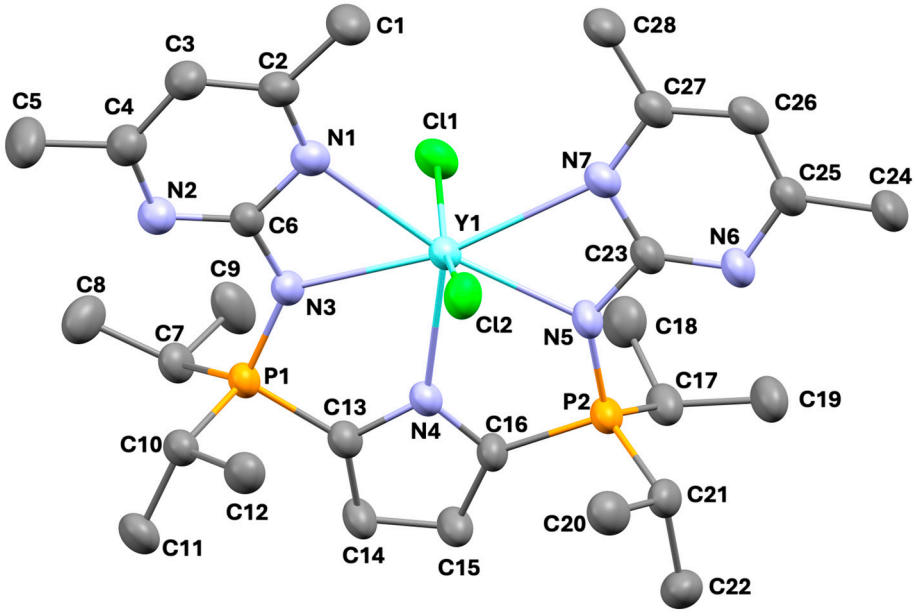

Figure 1. The molecular structure of $LYCl_2$·toluene. The anisotropic displacement ellipsoids are shown at the 50% probability level. Hydrogen atoms and the toluene solvent molecule are omitted for clarity.

Table 1. Selected geometric parameters of $LYCl_2$ and literature averages (Å, °).

Atom	Atom	Length/Å	Atom	Atom	Atom	Angle (°)
Y1	Cl1	2.6072(8)	Cl2	Y1	Cl1	161.81(3)
Y1	Cl2	2.6064(8)	N1	Y1	Cl1	82.66(6)
Y1	N1	2.567(2)	N1	Y1	Cl2	86.77(6)
Y1	N3	2.358(2)	N1	Y1	N7	114.17(8)
Y1	N4	2.375(2)	N3	Y1	Cl1	91.83(7)
Y1	N5	2.368(2)	N3	Y1	Cl2	93.83(7)
Y1	N7	2.584(3)	N3	Y1	N1	53.83(8)
			N3	Y1	N4	68.90(8)
	$LYCl_2$ Averages		N3	Y1	N5	138.46(8)
Y1	Cl_{ave}	2.6028 ± 0.0004	N3	Y1	N7	167.30(8)
Y1	N1/N7	2.576 ± 0.009	N4	Y1	Cl1	102.22(6)
Y1	N3/N5	2.363 ± 0.005	N4	Y1	Cl2	95.94(6)
			N4	Y1	N1	122.70(8)
	Literature Averages		N4	Y1	N7	123.07(8)
Y1	Cl	2.62 ± 0.02	N5	Y1	Cl1	98.01(6)
Y1	N3/N5	2.39 ± 0.02	N5	Y1	Cl2	89.15(6)
Y1	N4	2.345 ± 0.002	N5	Y1	N1	167.40(9)
Y1	N	2.5126 ± 0.009	N5	Y1	N4	69.58(8)
Lu1	N1/N7	2.546 ± 0.002	N5	Y1	N7	53.81(8)
Zr1	N	2.479 ± 0.008	N7	Y1	Cl1	81.71(6)
Zr1	Cl	2.25 ± 0.05	N7	Y1	Cl2	89.24(6)

When comparing bond lengths to yttrium, it is noteworthy that there are no other examples within the CSD of seven-coordinate yttrium dichloride complexes bearing a pentadentate ligand comprised entirely of nitrogen donors. Comparison of Y–Cl distances within the CSD were predominantly restricted to seven-coordinate yttrium complexes with two chlorides and five nitrogen donors from multiple ligands [AXACOR [13], KOHQIK [14], LIJJOF [15], NIRKOQ [16], ZUNLOJ [17], ZUNLUP [17]]. An yttrium complex supported by a related ancillary ligand [ROGFOK [2]] was used as the comparison for the expected average Y–N4 and Y–N3/N5 bond lengths. The two bonds between the metal center and the pyrimidine nitrogen donors (Y1–N1 and Y1–N7) were compared to those in the analogous lutetium complex (Lu1–N1/N7), $LLuCl_2$ [XUYGIL [12]], as well as the average Y–N distances in a cationic seven-coordinate yttrium complex bearing five nitrogen-donor ligands [XILPUH [18]]. In addition, the average Zr1–N and Zr1–Cl lengths in zirconium dichloride species supported by five nitrogen donors [BUPBEU, BUPBOE [19]] were scrutinized. As expected, the examined distances were slightly shorter than those in $LYCl_2$, consistent with periodic trends. The geometrical parameters of $LYCl_2$ and the comparative literature average bond lengths are provided in Table 1.

2.2. Supramolecular Features

The title compound crystallized in the monoclinic space group I2/a with one disordered toluene molecule. Symmetry elements, including 2_1 screw and 2-fold axes perpendicular to the b-axis, inversion centers between molecules, and c-glides at y = 0.25, 0.5, and 0.75, relate each yttrium complex to one another.

Although there are several short intermolecular contacts, those addressed in this work have been limited to contacts shorter than the sum of the VdW radii minus 0.20 Å (Figure 2, Table 2). There is only one such contact between the toluene molecule and the yttrium complex, an interaction between a hydrogen atom on an isopropyl group and a toluene ring hydrogen (H5T···H22C′). Another short contact exists between the pyrrole and pyrimidine

carbons (C3···C15′), and as does one between the chloride ligand and a methyl hydrogen on the pyrimidine group (Cl2···H5B′). Notably, there are no short contacts involving yttrium.

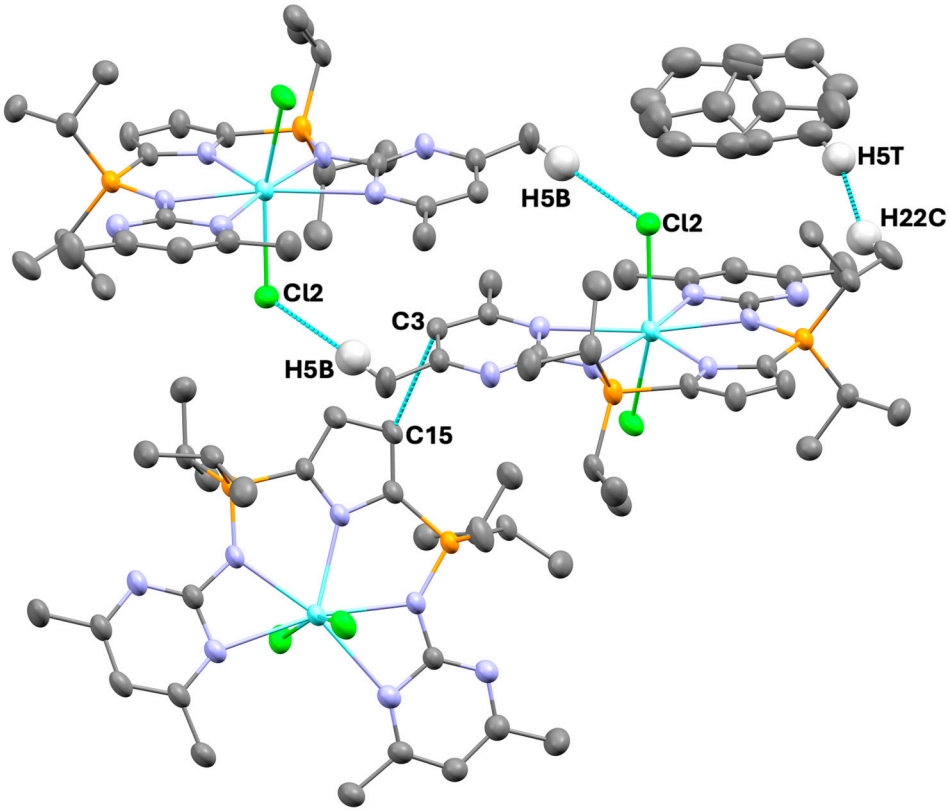

Figure 2. Dashed lines in blue indicate short intermolecular and close contacts (shorter than the VdW radii minus 0.20 Å). For clarity, hydrogen atoms are not shown. The disordered (72.5:22.5 occupancy) toluene of crystallization is included at the top right.

Table 2. Summary of contacts (Å) that are shorter than the sum of the VdW radii minus 0.20 Å.

Number	Atom 1	Atom 2	Length	Length-VdW	Symm. Op. 1	Symm. Op. 2
1	C3	C15′	3.317	−0.223	x, y, z	−1/2 + x, 1−y, z
2	Cl2	H5B′	2.598	−0.422	x, y, z	1/2 − x, 1/2 − y, 1/2 − z
3	H22C	H5T′	2.161	−0.239	x, y, z	x, y, z

3. Materials and Methods

3.1. General Methods

Manipulation of air- and moisture-sensitive reagents was carried out under an argon or dinitrogen atmosphere in an MBraun glove box or vacuum line. Solvents (THF and toluene) were purified using an MBraun solvent purification system, dried over 4 Å molecular sieves, degassed via three freeze–pump–thaw cycles, and further stored in glass bombs over sodium benzophenone. All solvents were distilled at the time of use. Benzene-d_6 was dried over sodium benzophenone, degassed via three freeze–pump–thaw cycles, distilled in vacuo and stored in a glass bomb under argon. All NMR spectra were recorded at ambient temperature with a Bruker Avance III NMR spectrometer. Chemical shifts are reported in parts per million (ppm) relative to the external standards $SiMe_4$ (^{1}H and ^{13}C) and 85% H_3PO_4 (^{31}P), and internal standard benzene-d_6 (^{1}H and ^{13}C). The synthesis of NaL followed a modified Staudinger reaction, which was previously reported by the Hayes

group [12]. $YCl_3(THF)_{3.5}$ was synthesized according to literature methods [20] from YCl_3, which was purchased from Sigma Aldrich without further purification.

3.2. Synthesis

Over a period of 10 min at ambient temperature, a THF (15 mL) solution of NaL (0.1115 g, 0.1934 mmol) was added dropwise to a stirring THF (15 mL) solution of $YCl_3(THF)_{3.5}$ (0.0855 g, 0.2077 mmol) in a round-bottomed flask attached to a swivel frit apparatus. After 3 h the THF was removed in vacuo, yielding a yellow-orange powder. Toluene (10 mL) was distilled into the reaction flask and the mixture was allowed to warm to ambient temperature. The solution was filtered to remove NaCl, then dried in vacuo, affording a yellow powder (0.1253 g, 0.1789 mmol, 92.5%). ^{1}H NMR (benzene-d_6, 23 °C, 700.44 MHz) δ: 6.68 (s, 2 H, pyrrole *H*), 5.86 (s, 2 H, pym aryl *H*), 2.61 (m, 4 H, PC*H*$(CH_3)_2$), 2.45 (s, 6 H, pym methyl *H*), 2.04 (s, 6 H, pym methyl *H*), 1.28 (dd, 12 H, $^3J_{HP}$ = 16.9, $^3J_{HH}$ = 7.1 Hz, PCH(C*H*$_3$)(CH$_3$)), 1.06 (dd, 12 H, $^3J_{HP}$ = 17.3, $^3J_{HH}$ = 7.1 Hz, PCH(CH$_3$)(C*H*$_3$)). ^{13}C{^{1}H} NMR (benzene-d_6, 23 °C, 176.13 MHz) δ 168.6 (s, pym ipso *C*) δ: 165.8 (d, $^2J_{CP}$ *J* = 4.8 Hz, pyrrole ipso *C*), 165.0 (s, pym ipso *C*), 119.2–115.5 (ov m, aromatic pyrrole *C*), 111.1 (s, pym aryl *C*), 25.6 (d, $^1J_{CP}$ = 54.0 Hz, PCH$(CH_3)_2$), 23.9 (s, pym methyl *C*), 23.5 (s, pym methyl *C*), 16.7 (s, PCH(*C*H$_3$)(CH$_3$)), 15.8 (s, PCH(CH$_3$)(*C*H$_3$)). ^{31}P{^{1}H} NMR (benzene-d_6, 23 °C, 283.54 MHz) δ 49.7.

3.3. Crystallization and Refinement

Single crystals of $C_{35}H_{52}Cl_2N_7P_2Y$ were obtained from a saturated toluene solution kept at −35 °C for 72 h. A suitable crystal was selected and mounted in Paratone oil using a 200 μm MiTeGen support on a SuperNova, Dual, Cu at home/near, Pilatus 200 K diffractometer. The crystal was kept at 100.00(10) K during data collection. Using Olex2 (version 1.5) [21], the structure was solved with the SHELXT (version 2018/2) [22] structure solution program using Intrinsic Phasing and refined with the SHELXL (version 2018/3) [23] refinement package using Least Squares minimisation. One molecule of toluene co-crystallized with each $LYCl_2$. This was found to be disordered, and was modelled with two parts that refined to 77.5:22.5 occupancy ratios. Interestingly, the disorder was not about a symmetry element. Hence, it was found necessary to restrain the minor component to the same bond distances as the major, and the ellipsoids of the minor were also constrained to be the same as in the major component. CCDC (deposit number 2486570) contains the supplementary crystallographic data for this paper. These data can be obtained free of charge Via http://www.ccdc.cam.ac.uk/conts/retrieving.html (or from the CCDC, 12 Union Road, Cambridge CB2 1EZ, UK; Fax: +44 1223 336033; E-mail: deposit@ccdc.cam.ac.uk).

Crystal Data for $C_{35}H_{52}Cl_2N_7P_2Y$, M = 792.58 g mol^{-1}, colourless plate, crystal dimensions 0.277 × 0.277 × 0.136 mm, monoclinic, space group I2/a (no. 15), a = 19.6238(2) Å, b = 13.3465(2) Å, c = 30.9453(4) Å, β = 99.6000(10)°, V = 7991.35(18) Å^3, Z = 8, T = 100.00(10) K, μ(Cu Kα) = 4.298 mm^{-1}, Dcalc = 1.318 g/cm^3, 40,233 reflections measured (5.794° ≤ 2Θ ≤ 149.924°), 8049 unique (R_{int} = 0.0571, R_{sigma} = 0.0406) which were used in all calculations. The final R_1 was 0.0425 (I > 2σ(I)) and wR_2 was 0.1165 (all data), with a goodness of fit on F^2 of 1.035.

Supplementary Materials: The following supporting information are available. Table S1. Crystal data and structure refinement; Table S2. Fractional Atomic Coordinates (×10^4) and Equivalent Isotropic Displacement Parameters (Å^2 × 10^3). U_{eq} is defined as 1/3 of the trace of the orthogonalised U_{IJ} tensor; Table S3. Anisotropic Displacement Parameters (Å^2 × 10^3). The Anisotropic displacement factor exponent takes the form: -2π^2[h^{2}a*^{2}U$_{11}$+2hka*b*U$_{12}$+…]; Table S4. Bond Lengths; Table S5. Bond Angles; Table S6. Torsion Angles; Table S7. Hydrogen Atom Coordinates (Å × 10^4) and Isotropic Displacement Parameters (Å^2 × 10^3); Table S8. Atomic Occupancy; Figure S1. ^{1}H NMR

spectrum (700 MHz) of $LYCl_2$ in benzene-d_6 at 22 °C; Figure S2. $^{13}C\{^1H\}$ NMR spectrum (176 MHz) of $LYCl_2$ in benzene-d_6 at 22 °C; Figure S3. $^{31}P\{^1H\}$ NMR spectrum (284 MHz) of $LYCl_2$ in benzene-d_6 at 22 °C.

Author Contributions: E.L.T. contributed to methodology, investigation, formal analysis, data curation, writing—original draft, reviewing and editing. D.S. contributed to methodology, investigation, formal analysis, and data curation. P.G.H. contributed to methodology, formal analysis, conceptualization, project administration, supervision, writing—original draft, reviewing and editing, resources and funding acquisition. All authors have read and agreed to the published version of the manuscript.

Funding: This research was funded by a Discovery Grant from the Natural Sciences and Engineering Research Council (NSERC) of Canada (341687). The diffractometer at the University of Lethbridge X-ray Diffraction Facility was purchased by the University and the Faculty of Arts & Science.

Data Availability Statement: The data that support the findings of this study are available in the Supplementary Material of this article.

Acknowledgments: The authors acknowledge the Canada Foundation for Innovation and NSERC of Canada. P.G.H. thanks the University of Lethbridge for a Tier I Board of Governors Research Chair in Organometallic Chemistry. René T. Boeré is gratefully acknowledged for support in data analysis, the publication process, and expert knowledge throughout the development of this manuscript. Thamara Salazar-Barrientos is appreciatively acknowledged for data acquisition.

Conflicts of Interest: The authors declare no conflicts of interest. The funders had no role in the design of the study; in the collection, analyses, or interpretation of data; in the writing of the manuscript; or in the decision to publish the results.

References

1. Piers, W.E.; Emslie, D.J.H. Non-cyclopentadienyl ancillaries in organogroup 3 metal chemistry: A fine balance in ligand design. *Coord. Chem. Rev.* **2002**, *233*, 131–155. [CrossRef]
2. Zamora, M.T.; Johnson, K.R.D.; Hanninen, M.M.; Hayes, P.G. Differences in the cyclometallation reactivity of bisphosphinimine-supported organo-rare earth complexes. *Dalton Trans.* **2014**, *43*, 10739–10750. [CrossRef]
3. Johnson, K.R.D.; Hayes, P.G. Synthesis and reactivity of dialkyl lutetium complexes supported by a novel bis(phosphinimine)carbazole pincer ligand. *Organometallics* **2009**, *28*, 6352–6361. [CrossRef]
4. Johnson, K.R.D.; Hannon, M.A.; Ritch, J.S.; Hayes, P.G. Thermally stable rare earth diakyl complexes supported by a novel bis(phosphinimine)pyrrole ligand. *Dalton Trans.* **2012**, *41*, 7873–7875. [CrossRef]
5. Knott, J.P.; Hanninen, M.M.; Rautianinen, J.K.; Tuononen, H.M.; Hayes, P.G. Insights into the decomposition pathway of a lutetium alkylamido complex via intramolecular C–H bond activation. *J. Organomet. Chem.* **2017**, *845*, 135–143. [CrossRef]
6. Summerscales, O.T.; Gordon, J.C. Complexes containing multiple bonding interactions between lanthanoid elements and main-group fragments. *RCS Adv.* **2013**, *3*, 6682–6692. [CrossRef]
7. Lu, E.; Li, Y.; Chen, Y. A scandium terminal imido complex: Synthesis, structure and DFT studies. *Chem. Commun.* **2010**, *46*, 4469–4471. [CrossRef]
8. Lu, E.; Chu, J.; Chen, Y. Scandium Terminal Imido Chemistry. *Acc. Chem. Res.* **2018**, *51*, 557–566. [CrossRef] [PubMed]
9. Li, T.; Huang, D.; Zhu, M.; Wei, J.; Zhang, W.X. Synergism between cyclopentadienyl and amidinate ligands affording anionic scandium terminal imido complexes. *Inorg. Chem. Front.* **2025**, *12*, 3791–3799. [CrossRef]
10. Lu, E.; Chu, J.; Chen, Y.; Borzov, M.V.; Li, G. Scandium terminal imido complex induced C-H bond selenation and formation of an Sc-Se bond. *Chem. Commun.* **2011**, *47*, 743–745. [CrossRef]
11. Schädle, D.; Meermann-Zimmermann, M.; Schädle, C.; Maichle-Mössmer, C.; Anwander, R. Rare-Earth Metal Complexes with Terminal Imido Ligands. *Eur. J. Inorg. Chem.* **2015**, *2015*, 1334–1339. [CrossRef]
12. Knott, J.P.; Hsiang, S.J.; Hayes, P.G. Alkylamido lutetium complexes as prospective lutetium imido precursors: Synthesis, characterization and ligand design. *Dalton Trans.* **2025**, *54*, 6261–6273. [CrossRef]
13. Roitershtein, D.; Domingos, Â.; Pereira, L.C.J.; Ascenso, J.R.; Marques, N. Coordination of 2,2′-Bipyridyl and 1,10-Phenanthroline to Yttrium and Lanthanum Complexes Based on a Scorpionate Ligand. *Inorg. Chem.* **2003**, *42*, 7666–7673. [CrossRef]
14. Caballo, J.; Mena, M.; Pérez-Redondo, A.; Yélamos, C. Cyclopentadienyl yttrium complexes with the [{Ti(η^5-C_5Me_5)(μ-NH)}$_3$(μ_3-N)] metalloligand. *J. Organomet. Chem.* **2019**, *896*, 139–145. [CrossRef]
15. Caballo, J.; Carbó, J.J.; Mena, M.; Pérez-Redondo, A.; Poblet, J.M.; Yélamos, C. Redox-Active Behavior of the [{Ti(η^5-C_5Me_5)(μ-NH)}$_3$(μ_3-N)] Metalloligand. *Inorg. Chem.* **2013**, *52*, 6103–6109. [CrossRef] [PubMed]

16. Hoang, T.N.Y.; Humbert-Droz, M.; Dutronc, T.; Guénée, L.; Besnard, C.; Piguet, C. A Polyaromatic Terdentate Binding Unit with Fused 5,6-Membered Chelates for Complexing s-, p-, d-, and f-Block Cations. *Inorg. Chem.* **2013**, *52*, 5570–5580. [CrossRef]
17. Evans, W.J.; Shreeve, J.L.; Boyle, T.J.; Ziller, J.W. Coordination chemistry of N-methylimidazole with yttrium and cerium. *J. Coord. Chem.* **1995**, *34*, 229–239. [CrossRef]
18. Petersen, J.B.; Ding, Y.-S.; Gupta, S.; Borah, A.; McInnes, E.J.L.; Zheng, Y.-Z.; Murugavel, R.; Winpenny, R.E.P. Electron Paramagnetic Resonance Spectra of Pentagonal Bipyramidal Gadolinium Complexes. *Inorg. Chem.* **2023**, *62*, 8435–8441. [CrossRef]
19. Bai, S.D.; Tong, H.B.; Guo, J.P.; Zhou, M.-S.; Liu, D.S.; Yuan, S.F. Diverse coordination behaviors of the silyl-linked bis(amidinate_ ligand $[SiMe_2\{NC(Ph)N(Ph)\}_2]^-$ to zirconium center. *Polyhedron* **2010**, *29*, 262–269. [CrossRef]
20. Sobota, P.; Utko, J.; Szafert, S. Ionization of YCl_3 in Tetrahydrofuran. Crystal Structures of the [*trans*-$YCl_2(THF)_5$][*trans*-$YCl_4(THF)_2$] Salt and Polymeric $[YCl_3 \cdot 2THF]_\infty$ Compounds. *Inorg. Chem.* **1994**, *33*, 5203–5206. [CrossRef]
21. Dolomanov, O.V.; Bourhis, L.J.; Gildea, R.J.; Howard, J.A.K.; Puschmann, H.J. OLEX2: A complete structure solution, refinement and analysis program. *J. Appl. Cryst.* **2009**, *42*, 339–341. [CrossRef]
22. Bourhis, L.J.; Dolomanov, O.V.; Gildea, R.J.; Howard, J.A.K.; Puschmann, H. The anatomy of a comprehensive constrained, restrained refinement program for the moderncomputing environment–Olex2 dissected. *Acta Cryst.* **2015**, *A71*, 59–75.
23. Sheldrick, G.M. SHELXT–Integrated space-group and crystal-structure determination. *Acta Cryst.* **2015**, *C71*, 3–8. [CrossRef] [PubMed]